

1 **Atmospheric moisture transport *versus* precipitation across the**
2 **Tibetan Plateau: a mini-review and current challenges**

3
4 **Yingzhao MA^{1,2}, Mengqian LU¹, Haonan CHEN^{3,4}, Mengxin PAN¹, Yang HONG^{2,5}**

5
6 *¹ Department of Civil and Environmental Engineering, The Hong Kong University of*
7 *Science and Technology, Kowloon, Hong Kong SAR 999077, China*

8 *² State Key Laboratory of Hydrosience and Engineering, Department of Hydraulic*
9 *Engineering, Tsinghua University, Beijing 100084, China*

10 *³ NOAA/Earth System Research Laboratory, Boulder, CO 80305, USA*

11 *⁴ Colorado State University, Fort Collins, CO 80523, USA*

12 *⁵ School of Civil Engineering and Environmental Sciences, University of Oklahoma,*
13 *Norman, OK 73019, USA.*

14
15 The Revised Manuscript Submitted to *Atmospheric Research*

16 *March, 2018*

17 ***Corresponding author address: Yingzhao MA, 2200A, Department of Civil and Environmental***
18 ***Engineering, The Hong Kong University of Science and Technology, Kowloon, Hong Kong SAR,***
19 ***China. E-mail: yingzhao.ma@gmail.com***

20

Abstract

21 The Tibetan Plateau (TP), being an average of surpassing 4000 *m* above sea level
22 and around $2.5 \times 10^6 \text{ km}^2$, is the highest and largest plateau in the world and also
23 called as the “Third Pole”. Due to its elevated land surface and complex terrain,
24 the TP is subjected to combined regulations of multiple climate systems and
25 associated large-scale atmospheric circulations. In this paper, we comprehensively
26 review the recent studies of atmospheric moisture transport *versus* precipitation
27 across the TP, with the attempt to link the two, which did not receive much
28 attention previously. This review focuses on the atmospheric moisture transport
29 and associated circulation patterns in this region, widely adopted approaches to
30 identify the atmospheric moisture transport, qualitative and quantitative analyses
31 for the role of water vapor transport on the precipitation, as well as the internal
32 physical mechanism between atmospheric moisture transport and precipitation
33 over the TP. Moreover, directions of future research are discussed based on the
34 following aspects, which include 1) proposing an integrated statistical-physical
35 framework for demonstrating the influence of atmospheric moisture transport and
36 associated circulation patterns on the precipitation, especially the extremes, in the
37 high-cold mountainous region; 2) quantifying the contribution of atmospheric
38 water vapor from the surrounding sources as well as the local moisture recycling
39 on the TP’s precipitation; 3) providing higher quality data for atmospheric water
40 vapor and precipitation; 4) emphasizing on the physical mechanism sustaining the
41 atmospheric moisture transport as well as its potential influence on the extreme
42 precipitation, including amount, frequency, intensity and duration. It is expected

43 that this review will be beneficial for exploring the linkage between atmospheric
44 moisture transport *versus* precipitation across the TP.

45 **Key words:** atmospheric moisture transport; precipitation; mini-review and
46 challenges; qualitative and quantitative analyses; Tibetan Plateau;

47 1. Introduction

48 The Tibetan Plateau (TP), with an average elevation of more than 4000 *m* above
49 sea level (*a.s.l.*), is the highest and largest plateau around the world. Give the
50 significance of climate change, the TP, accompanied with Antarctic and Arctic, is
51 currently attracting increased attention by the academic community ([Qiu, 2008](#)).
52 Due to its unique terrain and specific underlying surfaces, the TP is subjected to
53 combined regulations by multiple climatic systems, where the circulation patterns
54 are featured primarily by the Indian monsoon in summer and the mid-latitude
55 Westerlies in winter, as well as the East Asian monsoon affecting the eastern
56 margin, e.g. Mount Gongga and eastern Qilian mountains ([Yao et al., 2012](#)). Also,
57 the TP is the source region of several major rivers in the Asian continent and
58 recognized as the “Asia’s water tower”, providing water for more than 1/3 of the
59 world’s population over China and India ([Xu et al., 2008](#); [Yao et al., 2012](#)). Thus,
60 an understanding of the nature and intensity of the hydrological cycle over the TP
61 and of its development over time is a topic of crucial importance. In particular,
62 precipitation, being a critical component of the water cycle, is one of the most
63 emerging challenges faced by scientists over the TP due to the lack of reliable high-
64 quality data set. ([Gimeno et al., 2012](#); [Ma et al., 2015](#); [Wang et al., 2017a](#)).

65 [Wang et al. \(2017a\)](#) reviewed the changes of the TP’s precipitation over the past
66 decades from the perspectives of observations and simulations. Overall, the

67 precipitation exhibits an increasing trend with moderate variability since 1960s in
68 the TP. Spatially, the precipitation shows a decreasing trend from southeast to
69 northwest. It also has a strong seasonality-primarily occurs in summer (from June
70 to August), accounting for nearly 70% of the annual total amounts ([Ma et al., 2016](#);
71 [Tong et al., 2014](#)). As the TP is a stronger heat source for the atmosphere in summer,
72 the convective activity is frequent at the sub-daily scale, especially in the late
73 afternoon. Thus, diurnal variation is significant for the precipitation in this region,
74 in particular over the hilly areas ([Maussion et al., 2014](#); [Xu et al., 2014](#)). Moreover,
75 the rainfall peak often occurs over the large lakes in the morning but the time of
76 peak rain rate is delayed as the lake size increases ([Singh and Nakamura, 2009](#)).
77 Thanks to the availability of more satellite products, *in-situ* observations, and
78 reanalysis simulations, more studies have been done recently to investigate the
79 precipitation variabilities and trends in the TP ([Gao and Liu, 2013](#); [Ma et al., 2016](#);
80 [Ma et al., 2015](#); [Maussion et al., 2014](#); [Shen et al., 2014](#); [Tong et al., 2014](#); [You et al.,](#)
81 [2015](#)).

82 The precipitation over the TP is significantly influenced by the variations of the
83 large-scale atmospheric circulations and associated local moisture recycling ([Chen](#)
84 [et al., 2012](#); [Curio et al., 2015](#); [Xu et al., 2014](#)). The local moisture recycling provides
85 higher atmospheric water vapor needed for the precipitation amounts than that
86 from the outside of the TP ([Curio et al., 2015](#)). But the remote moisture transports,
87 which are driven by the large-scale atmospheric circulations, primarily influence
88 the variability of summer precipitation over the TP ([Feng and Zhou, 2012](#); [Wang](#)
89 [et al., 2017b](#)). Given the projected global warming in the future, the atmospheric
90 water vapor holding capacity is expected to increase with elevated temperature,

91 potentially causing changes of precipitation features in terms of intensity and/or
92 frequency ([Xu et al., 2008](#)). Thus, more attentions are paid to explore the role of
93 atmospheric moisture transport on the precipitation as well as its internal physical
94 mechanisms across the TP in recent years ([Cannon et al., 2016](#); [Curio et al., 2015](#);
95 [Dong et al., 2016](#); [Feng and Zhou, 2012](#); [Wang et al., 2017b](#); [Xu et al., 2008](#); [Zhang](#)
96 [et al., 2017](#)). Various studies have been done in other regions, exemplified by the
97 North and South America, the Europe and the Southeast China ([Gershunov et al.,](#)
98 [2017](#); [Gimeno et al., 2010](#); [Gimeno et al., 2014](#); [Gimeno et al., 2012](#); [Hecht and](#)
99 [Cordeira, 2017](#); [Lamjiri et al., 2017](#); [Lavers and Villarini, 2013](#); [Lu and Hao, 2017](#);
100 [Lu and Lall, 2017](#); [Lu et al., 2013](#); [van der Ent et al., 2010](#)).

101 In summary, recent studies have deepened our understanding on the origin and
102 evolution of the precipitation in the TP, ranging from some early-stage qualitative
103 assessment to subsequently more integrated quantitative analysis. And related
104 topics have been explored in other regions of the world, providing a good
105 foundation for our investigation in the TP. However, a thorough review and a
106 comprehensive summary is urgent to advance the knowledge of the role of
107 atmospheric moisture transport and associated circulation patterns on the TP's
108 precipitation, especially given the recent trend of the increasing extreme
109 hydrometeorological events in this high-elevated region ([Donat et al., 2016](#);
110 [Ingram, 2016](#); [Kang et al., 2010](#); [You et al., 2008](#)).

111 The paper is organized as follows. Section 2 describes recent research progress
112 of atmospheric water vapor and its link with precipitation across the TP, from the
113 atmospheric moisture transport and associated circulation patterns (Section 2.1),
114 to the widely adopted approaches for prominent moisture transport detection

115 (Section 2.2), then followed by some analysis of their roles in the TP precipitation
116 (Section 2.3 & 2.4) and the governing physical mechanism (Section 2.5). Further
117 challenges and prospects are discussed in Section 3. The conclusion is summarized
118 in Section 4 at the end.

119 **2. Recent processes of atmospheric moisture transport *versus* precipitation** 120 **across the TP**

121 **2.1 Atmospheric moisture transport and associated circulation patterns in a** 122 **changing climate**

123 The upper-level atmospheric moisture transport plays an important role in the
124 entire global natural and climate environment ([Waliser et al., 2012](#)). Filamentary
125 structure is a common feature for the atmospheric moisture transport (Figure 1).
126 At any time, three-to-five typically major conduits exist in each hemisphere, and
127 each belt with the length more than 2000 km and width ranging from 500 to 1000
128 km carries large amounts of moisture across the mid-latitudes ([Zhu and Newell,](#)
129 [1994](#); [Zhu and Newell, 1998](#)). A great number of convey belts are observed in the
130 north-eastern Pacific, and about 15 land-falling convey belts per year are counted
131 in California over longer periods and 8-10 consistent winter filaments affect winter
132 floods in Britain ([Hecht and Cordeira, 2017](#); [Lavers and Villarini, 2013](#); [Lavers et](#)
133 [al., 2012](#); [Neiman et al., 2008](#); [Waliser et al., 2012](#)). Other major global moisture
134 sources in the tropical Atlantic oceanic areas are found to be linked with extreme
135 precipitation in the Northeastern United States, the Southeastern China and the
136 Western Europe ([Lu and Hao, 2017](#); [Lu and Lall, 2017](#); [Lu et al., 2013](#)). Thus,
137 enhanced atmospheric moisture transports clearly contribute to the occurrence of
138 hydrological extremes in many regions over the globe.

139 As the Asia's water tower, there are four primary climate systems regulating
140 the moisture transport to the TP, including the Indian monsoon system, the mid-
141 latitude Westerlies, the East Asian monsoon system and the local moisture
142 recycling (also termed as "Tibetan Plateau monsoon") (Figure 2) ([Bolch et al., 2012](#);
143 [Duan et al., 2011](#); [Tang and Reiter, 1984](#); [Tian et al., 2007](#); [Xu et al., 2008](#); [Yao et al.,](#)
144 [2012](#)). The elevated topography of the TP is taken as a barrier to the mid-latitude
145 Westerlies and also enhances the Indian monsoon through its dynamical and
146 thermal driving forces, thus contribute to the large-scale atmospheric circulations.
147 Since there is a strong contrast of thermal property between land and ocean, a
148 seasonally cross-south-north hemispherical monsoonal circulation exists in the
149 earth. In summer, the TP serves as a strong "dynamic pump" and continuously
150 attracts moist air from the surrounding oceans through deep canyons in the
151 southern and western boundaries, even if their western boundary is further east
152 ([Feng and Zhou, 2012](#); [Xu et al., 2008](#)). The water vapor entering the TP through
153 the eastern part of the southern margin is from the Indian monsoon air masses,
154 while that through the western margin originates from the mid-latitude Westerlies.
155 Revealed from the oxygen isotopes in precipitation, [Tian et al. \(2001\)](#) showed that
156 the atmospheric moisture transport trajectories originate from the Arabian Sea to
157 Indian continent, then to the Bay of Bengal, and finally arrive at the TP in summer.
158 Based on the numerical experiments, [Sugimoto et al. \(2006\)](#) demonstrated that the
159 process of water vapor transport into the TP contains multiple steps: the Westerlies
160 carry the water vapor to the southern foot of the Himalayas at 1500 *m a.s.l.* in the
161 afternoon, and then upslope winds in the southern slopes of the Himalayas convey
162 the moist air mass to the plateau level.

163 Since the TP is a strong heat source in summer, the local moisture recycling
164 forced by the thermal effect impacts the summer rainfall associated with
165 atmospheric circulations in the internal TP ([Duan et al., 2011](#); [Kurita and Yamada,
166 2008](#)). However, the thermal forcing may not be the primary factor for regulating
167 the TP's precipitation variability. [Wang et al. \(2017b\)](#) found that remote moisture
168 transport controls the variability of summer precipitation over the southern TP.
169 There is also a persistent anticyclone over the Arabian Sea along the Somalia coast
170 in winter, which takes more water vapor into the subtropical jet. The further
171 moistened Westerlies jet continues to transport water vapor into the TP ([Xu et al.,
172 2008](#)).

173 **2.2 Several approaches to identify atmospheric moisture transport**

174 Several features of the moisture transport, such as water vapor content, wind
175 speed and the shape of intensive moisture fluxes, etc., influence the precipitation,
176 especially for extreme rainfall. ([Gimeno et al., 2014](#); [Gimeno et al., 2012](#); [Knippertz
177 et al., 2013](#); [Waliser et al., 2012](#)). To clarify how atmospheric moisture transport
178 influences the precipitation variability, the distribution and movement of water
179 vapor need to be quantified first using satellite retrievals and/or ground-based
180 observations.

181 There are four widely adopted approaches to retrieve the characteristics of
182 atmospheric moisture transport, which are 1) using the vertically integrated water
183 vapor transport fluxes (IVT) between the surface pressure and the pressure limit
184 at the highest altitude of reliable radiosonde measurements ([Zhu and Newell,
185 1998](#)), 2) calculating the distribution of Integrated Water Vapor (IWV) from multi-
186 sources/sensors or reanalysis model simulations ([Dettinger et al., 2011](#); [Neiman et](#)

187 [al., 2008](#); [Ralph et al., 2004](#)), 3) estimating the Tropical Moisture Exports (TMEs)
 188 using the Lagrangian analysis on the basis of several-day forward trajectories
 189 starting from tropical lower troposphere ([Knippertz and Wernli, 2010](#); [Knippertz](#)
 190 [et al., 2013](#)), 4) analyzing the stable oxygen isotope in precipitation which can be
 191 obtained from either field observations or isotopic atmospheric circulation models
 192 ([Tian et al., 2007](#); [Yao et al., 2013](#)).

193 The IVT is calculated from the water vapor mixing ratios, i.e., the specific
 194 humidity (q , unit: kg/kg) and the zonal and meridional wind components (u and
 195 v , respectively, unit: m/s) for the troposphere, i.e., from the surface (1000 hPa) or
 196 all mandatory-level pressure surfaces (p_0) up to the pressure limit at the highest
 197 altitude of reliable radiosonde measurements (300 hPa). The product components
 198 $q \times u \times dp/g$ and $q \times v \times dp/g$ at each grid point were summed vertically from
 199 the surface to 300 hPa and then combined into a horizontal transport vector, with
 200 units of $kg\ m^{-1}\ s^{-1}$ below ([Neiman et al., 2008](#); [Zhu and Newell, 1998](#)).

$$201 \quad IVT = \sqrt{\left(\frac{1}{g} \int_{p_0}^{300} qu dp\right)^2 + \left(\frac{1}{g} \int_{p_0}^{300} qv dp\right)^2} \quad (1)$$

202 Since there is not a universal threshold for the identification of atmospheric
 203 rivers or deeper corridors with concentrated water vapor transports from the
 204 aforementioned literatures, the percentiles of the IVT distribution instead of a
 205 single value is preferred for different regions ([Lavers et al., 2012](#)). The detection
 206 approach is typically on the basis of a zonal threshold ([Zhu and Newell, 1998](#)), or
 207 a zonal and meridional threshold ([Jiang and Deng, 2011](#)). For instance, [Lavers and](#)
 208 [Villarini \(2013\)](#) used the 85th percentile of the IVT in each latitude bin as the
 209 threshold for identifying the atmospheric rivers in the pan-European region. In

210 addition to the IVT threshold, some features, including time step, search region,
211 latitudinal movement and time interval of the IVT maximum, are also considered.
212 Further details and discussion of this method can be found in [Lavers and Villarini](#)
213 [\(2013\)](#); [Lavers et al. \(2012\)](#); [Zhu and Newell \(1998\)](#).

214 It is well known that a key contributor to the advection of water vapor is the
215 low-level jet, also referred to as the “warm conveyor belt”. Since there is a close
216 correlation between horizontal water vapor flux and the horizontal distribution of
217 integrated water vapor (IWV) at each grid point, the IWV is considered as a proxy
218 to characterize narrow features describing most of the instantaneous meridional
219 water vapor transport at mid-latitudes ([Schluessel and Emery, 1990](#)). [Ralph et al.](#)
220 [\(2004\)](#) indicated that 75% of the observed fluxes through a 1000 *km* cross-front
221 baseline includes a 565 *km* width zone roughly 4 *km* depth, and the meridional
222 water vapor flux is 1.5×10^8 *kg/s*. The IWV takes into account the density of liquid
223 water, which expressed in *kg/m²* and also labeled as *mm* of total precipitable water.
224 It is the vertically integrated total mass of water vapor *per* unit area for a column
225 of atmosphere. The IWV formula is given below:

$$226 \quad \text{IWV} = \int_{z=0}^z \rho_v(z) dz \quad (2)$$

227 where *z* refers to the column of atmosphere water vapor, and ρ_v is absolute
228 humidity, the same as the water vapor density. However, not all the water vapor
229 is actually precipitable. Gimeno et al. (2014) presented an approach of applying
230 the criteria on the IWV, e.g., in terms of the areas greater than 2 *cm*, narrower than
231 1000 *km*, and longer than around 2000 *km*, as well as the wind speed in the lowest
232 2 *km* greater than 12.5 *m/s*. However, the above characteristics are summarized in

233 the North American west coast, and they should be carefully redefined in other
234 regions, such as the TP. Because of the strong water vapor absorption near 22GHz
235 in the microwave range, the IWV can be retrieved using the classical radiative
236 transfer model and careful instrument intercalibration from microwave sensor,
237 such as SSM/I, SSMIS, TMI, AMSR-E, WindSat, AMSR2, GMI ([Hou et al., 2014](#);
238 [Neiman et al., 2008](#); [Ralph et al., 2004](#); [Schuessel and Emery, 1990](#)). Because of
239 frequent blockage by the rainfall, the vertical wind profile is difficult to quantify
240 from the current satellite estimates. Thus, it is challenging for the IWV to quantify
241 as a proxy for the identification of atmospheric moisture structures.

242 The Lagrangian method is also developed to quantify the contribution of the
243 atmospheric moisture transport to the precipitation coupled with air parcels by
244 backward or forward trajectories. It is recommended by [Knippertz and Wernli](#)
245 [\(2010\)](#) to propose an objective climatology of TMEs from more than 1.25 billion
246 trajectories using the reanalysis data sets. The trajectories are calculated with the
247 Lagrangian Analysis Tool (LAGRANTO), which is widely used in the atmospheric
248 sciences, for instance to identify flow structures in extratropical cyclones and long-
249 range transport pathways of moisture and trace substances ([Sprenger and Wernli,](#)
250 [2015](#); [Werner and Davies, 1997](#); [Wernli, 1997](#)). The identification process of TMEs
251 includes three steps: 1) to define the moisture source in the tropics between 0 and
252 20°N, and between 1000 *hPa* and 490 *hPa*, since about 90% of all the water vapor is
253 concentrated below the level of 490 *hPa*. However, it is noted that these trajectories
254 might be not appropriate in regions of active tropical convection ([Knippertz and](#)
255 [Wernli, 2010](#)); 2) to quantify the poleward circulation, where only the trajectories
256 crossed the 20°N are considered for another six days, and if they have reached

257 35°N within this period, they are retained. The average meridional wind speed
258 must exceed 2.85 m/s ; 3) to diagnose the significant moisture transport into the
259 extratropics, and only retain those trajectories that have moisture flux exceeding
260 $100 g kg^{-1} m s^{-1}$ in the north of 35°N. In general, the number of trajectories varies
261 nonlinearly with the selected threshold. Such a flux for the threshold of $100 g kg^{-1}$
262 $m s^{-1}$ is more feasible for “fast” or “robust” trajectory events with meaningful
263 statistics test ([Knippertz and Wernli, 2010](#)). However, this approach does not
264 quantify the uptake of water vapor along the track. In addition, the influence of
265 ocean evaporation along the subtropical area on TMEs trajectories is not specially
266 involved ([Knippertz et al., 2013](#)). Trajectory analysis of air parcels has gained a lot
267 popularity for the past two decades. Many trajectory analysis tools are developed
268 for computing backward and forward trajectories using reanalysis data sets. These
269 tools include FLEXTRA ([Stohl, 1998](#)), the NASA Goddard trajectory model
270 ([Schoeberl and Newman, 1995](#)), the Hybrid Single-Particle Lagrangian Integrated
271 Trajectory model (HYSPLIT) ([Draxler and Hess, 1998](#); [Stein et al., 2015](#)), and the
272 UGAMP offline trajectory model ([Methven, 1997](#)). Moreover, the space-time
273 statistical analysis on the trajectory products have shown its contribution to better
274 understanding of the linkage between enhanced moisture transport and extremes,
275 especially in the mid-latitudes ([Lu and Hao, 2017](#); [Lu and Lall, 2017](#); [Lu et al., 2013](#);
276 [Najibi et al., 2017](#))

277 The isotopic composition of precipitation, e.g., observed and modelled stable
278 oxygen isotope ratios ($\delta^{18}O$), is another approach to identify the sources and
279 pathways of water vapor ([Cai and Tian, 2016](#); [Guo et al., 2017](#); [Yao et al., 2013](#)). For
280 example, Figure 3 displays the precipitation $\delta^{18}O$ monitoring network and

281 associated schematic framework of the main moisture processes over the TP. The
282 water isotope samples are collected at the field sites using a specifically designed
283 container to avoid the danger of sample re-evaporation ([Groning et al., 2012](#)). The
284 samples are then analyzed using the Liquid Water Isotope Analyzer (e.g., Picarro-
285 2130i) in the Lab ([Guo et al., 2017](#)). Moreover, three widely used isotopic
286 Atmospheric General Circulation Models (AGCMs-iso), i.e., LMDZ-iso, REMO5-
287 iso, and ECHAM5-wiso, provide the gridded water stable isotopes with high
288 spatial resolution and gain substantial new insights into the moisture transport
289 ([Hoffmann et al., 1998](#); [Risi et al., 2010](#); [Sturm et al., 2005](#)). However, the AGCMs-
290 iso are not capable of simulating the observed rapid and large variations of the
291 water isotope signals. Note that the integrations between the explicit samples of
292 precipitation isotopes and the simulations of the state-of-the-art AGCMs-iso
293 enable us to deeply understand the moisture transports.

294 **2.3 Qualitative analysis for the role of atmospheric moisture transport on** 295 **precipitation in the TP**

296 The TP's precipitation generally shows a slightly increasing trend in the past
297 decades under the warming climate ([Kang et al., 2010](#); [Ma et al., 2018b](#)). [Xu et al.](#)
298 [\(2008\)](#) reported a positive correlation between atmospheric moisture content and
299 precipitation during the past 50 years over the TP. According to the classical
300 Clausius-Clapeyron equation ([Trenberth, 2011](#)), the increasing temperature leads
301 to higher capacity of atmospheric moisture, and thus very likely results in more
302 precipitation. The large-scale atmospheric circulations dominate the water vapor
303 transport and thus regulate the interannual variability of summer precipitation
304 across the TP ([Chen et al., 2012](#); [Liu and Yin, 2001](#); [Xu et al., 2008](#)). Also, a seesaw

305 structure with regard to the interannual variability of summer precipitation is
306 identified between the southern and northern TP. It is closely associated with the
307 North Atlantic Oscillation [NAO] ([Liu and Yin, 2001](#)).

308 The TP, especially in the mountainous regions, has strong local precipitation
309 systems in summer ([Gou et al., 2018](#)), and locally recycled moisture also plays a
310 crucial role in the precipitation associated regional circulation. For instance, the
311 local recycling ratio, which is the contribution of locally evapotranspired water
312 in the boundary layer, increases from 30% to 80% as the regional circulation type
313 of rainfall occurs ([Kurita and Yamada, 2008](#)). [Chow and Chan \(2008\)](#) proposed that
314 the local forcing indices, such as strong solar radiation and complex terrains, might
315 dominate the summer rainfall patterns at the diurnal scale in the TP. The diurnal
316 cycle of summer rainfall is more associated with a robust diurnal cycle of the
317 atmospheric system around the southern TP, where a strong daytime wind
318 accompanied with increasing humidity prevails in the deep valleys ([Ueno et al.,
319 2008](#)). The southeasterly wind carries out favorable moisture for the midnight and
320 early morning rainfall ([Bhatt and Nakamura, 2006](#)). In addition, the cyclonic
321 circulation over the Indian subcontinent hampers parts of water vapor intrusion
322 into the TP ([Sugimoto et al., 2006](#)). However, the internal physical mechanism
323 needs further verifying with plenty of field observations.

324 The dominant origin of the moisture contributing to the TP is a narrowly
325 tropical-subtropical belt from the Indian subcontinent to the southern Hemisphere.
326 Another two sources are identified in the northwestern part of the TP and the Bay
327 of Bengal ([Chen et al., 2012](#)). The water vapor from the Bay of Bengal moves
328 through the Brahmaputra channel and plays a significant role on the precipitation

329 characteristics in the southeastern TP ([Maussion et al., 2014](#)). While the southwest
330 is more influenced by the water vapor from northern Indian subcontinent ([Dong
331 et al., 2016](#)). The shifting moisture origin between Bay of Bengal and southern
332 Indian Ocean influences the precipitation patterns in the southern TP, with an
333 abrupt decrease in May and most depletion in August in terms of precipitation
334 $\delta^{18}\text{O}$ ([Yao et al., 2013](#)).

335 **2.4 Quantitative analysis for the contribution of atmospheric moisture** 336 **transport to precipitation in the TP**

337 The contributions to the precipitation variability in the TP by the local
338 moisture recycling and the remotely water vapor transport are comparable ([Xu et
339 al., 2014](#)). A growing number of studies have been not only focused on identifying
340 water vapor origins but also quantifying their contributions to the precipitation in
341 the TP ([Curio et al., 2015](#); [Feng and Zhou, 2012](#); [Wang et al., 2017b](#); [Zhang et al.,
342 2017](#)).

343 [Feng and Zhou \(2012\)](#) initially examined the various sources of atmospheric
344 water vapor for summer precipitation over the southeastern TP during 1979-2002
345 using multiple reanalysis data. To quantitatively reveal the vertical distribution of
346 moisture transport, they divide the whole air column into lower (1000-700 *hPa*),
347 middle (700-400 *hPa*), and upper (400-300 *hPa*) layers across the four borders of the
348 TP. Overall, the moisture from the southern edge, which comes from the Indian
349 Ocean and the Bay of Bengal, dominates the summer precipitation in the
350 southeastern TP. Around 32% of the water vapor comes from the western part
351 along the southern margin of the TP. As for the interannual variability of summer
352 precipitation in the southeastern TP, it is dominated by the anomalous anticyclone

353 at the Bay of Bengal and the northern Indian subcontinent. An excessive rainfall
354 anomaly of 1 mm/day in this region is associated with an anomalous water vapor
355 input of $138 \text{ kg m}^{-1} \text{ s}^{-1}$ and $104 \text{ kg m}^{-1} \text{ s}^{-1}$ from the western and southern margins of
356 TP, respectively ([Feng and Zhou, 2012](#)).

357 Although a first step has attempted to quantify the water vapor's contribution
358 on the precipitation of the TP, the question arises of whether the high-resolution
359 data sets lead to an improvement on the atmospheric moisture quantitation. Later,
360 [Curio et al. \(2015\)](#) critically quantified the atmospheric moisture transport towards
361 the TP based on a new data set, i.e., the 12-year High Asia Refined analysis (HAR),
362 which better describes the complex topography of the TP. They concluded that
363 $36.8 \pm 6.3\%$ of the contributing atmospheric moisture comes from outside of the TP,
364 while local moisture recycling accounts for the remaining 63.2% . The mid-latitude
365 Westerlies contribute higher for the moisture transport in summer than previously
366 assumed. It shows that the Westerlies are not fully blocked by the TP and parts of
367 the moisture are redirected to the north/south.

368 [Wang et al. \(2017b\)](#) investigated the relative contribution of remote moisture
369 transport and local surface evaporation to the summer rainfall variability over the
370 southern TP. The averaged moisture flux and local surface evaporation in summer
371 are 4.16 mm/d and 2.79 mm/d from 1980 to 2010, respectively, which is consistent
372 with the observed average summer rainfall rate of 7.17 mm/d . That's to say, local
373 moisture recycling amounts to around 40% to the total summer rainfall over the
374 southern TP. The remote moisture transport regulates the interannual variability
375 in the summer rainfall in this region, since the mean anomaly of local surface
376 evaporation is merely 0.07 mm/d . For the remote moisture sources, the southern

377 and western boundaries are two incoming channels with moisture fluxes of
378 $1991.47 \text{ kg m}^{-1} \text{ s}^{-1}$ and $160.13 \text{ kg m}^{-1} \text{ s}^{-1}$, respectively. Both of the northern and eastern
379 boundaries are export channels with regard to the moisture fluxes in terms of
380 $267.77 \text{ kg m}^{-1} \text{ s}^{-1}$ and $381.97 \text{ kg m}^{-1} \text{ s}^{-1}$, respectively. Although most external moisture
381 comes cross the southern edge, it serves as a secondary contribution to the
382 variation of the summer rainfall in the southern TP. Because most of the moisture
383 is directly converted into precipitation during the elevating process over the steep
384 southern slope of the TP ([Lin et al., 2018](#); [Wang et al., 2017b](#)), the water vapor from
385 the western margin mainly regulates the summer rainfall variability in spite of its
386 relatively weaker total contribution.

387 The TP shows an overall wetting trend especially in the west-central TP during
388 the past decades. By using the modified Water Accounting Model, the changes in
389 the moisture sources of the precipitation in the west-central TP are quantitatively
390 investigated ([Zhang et al., 2017](#)). On average, the land and ocean contribute > 69%
391 and > 21% of the water vapor supply to the total precipitation in the targeted area,
392 respectively, while the local moisture recycling contributes around 18% of the total
393 precipitation. As for the recent increase of precipitation in the west-central TP, the
394 enhanced water vapor transport from the Indian Ocean in July and September and
395 the intensified local moisture recycling might be the dominating cause ([Zhang et](#)
396 [al., 2017](#)).

397 The quantitative analysis of atmospheric water transport from different areas
398 towards the TP relies on the calculation of the moisture budget through the cross
399 sections following the border of the TP. Given the accuracy of the data sources, the
400 position of the cross sections used to calculate the moisture budget, and the

401 vertical resolution of the data sets, as well as the reanalysis model structures, some
402 biases of the results might be introduced. Thus, the exploration of quantifying the
403 contribution of atmospheric moisture transport to the precipitation in the TP is still
404 on its early stage given the current progress and findings.

405 **2.5 Physical mechanism between atmospheric moisture transport and** 406 **precipitation in the TP**

407 The physical mechanism explaining the roles of water vapor transport and the
408 associated synoptic-scale circulation patterns in the TP's precipitation is
409 complicated ([Feng and Zhou, 2012](#)) and needs further diagnostic analysis. The
410 governing system is influenced by the Indian monsoon systems, the mid-latitude
411 Westerlies and the elevated heating of the plateau. The climate teleconnections,
412 including the NAO, the Indian Ocean Dipole (IOD) mode, and El Niño-Southern
413 Oscillation, have an additional effect on the climate monsoon systems at different
414 timescales ([Cherchi and Navarra, 2012](#); [Liu et al., 2015](#)), and in turn take a far-
415 reaching influence on the atmospheric moisture transport across the TP ([Lin et al.,](#)
416 [2016](#); [Wang et al., 2017b](#)).

417 The TP is a persistent pool of water vapor maximum in the 500-300 *hPa*
418 atmosphere layer, which is named as an "air pump" ([Xu et al., 2008](#)). There is a
419 strong thermal contrast between the TP and its surrounding oceans, and the water
420 vapor from the low-latitude oceans moves toward the elevated plateau by this air
421 pump ([Wu et al., 2012](#)). The convergence of the warm-moist air lifts along the
422 plateau's slope and diverges at the top height. Because the sucking and pumping
423 effects in the southern TP contribute most of the moisture ascent and convergence
424 in the monsoon season, heavy rainfall event is frequent across the Himalayas ([Wu](#)

425 [et al., 2007](#)). [Xu et al. \(2014\)](#) proposed that a two-ladders of “CISK-like mechanism”
426 (conditional instability of the second kind) forces water vapor flows climbing up
427 the southern slope of Himalayas (Figure 4). The thermodynamic processes depict
428 a coupling of two CISK type systems, both with convergence at low level and
429 divergence at upper level. But the coupled system is horizontally contiguous and
430 vertically staggered. The diverged flow drives the convergence at the low-pressure
431 center in the TP, provides the local convection system with warm-moist air, and
432 consequently results in precipitation over the TP.

433 Based on several lines of evidences based on satellite and in-situ observations,
434 numerical sensitivity simulations, and water vapor trajectories, [Dong et al. \(2016\)](#)
435 found that the pathway of moisture transport is “up-and-over” rather than by
436 “upslope” flow along the southern Himalayas (Figure 5). The hydrometers and
437 moist air parcels are lifted by convective storms over the Indian subcontinent and
438 the foothills of Himalayas, and subsequently swept along the southern edge by
439 the mid-tropospheric circulation. The “up-and-over” moisture transport accounts
440 for ~23% of the summertime and contributes to half of the total summer rainfall in
441 the southwestern TP.

442 **3 Research challenges and prospects**

443 The study on the atmospheric moisture transport and its linkage with the
444 precipitation over the TP has achieved great progress for the past decades.
445 However, more attention is suggested to devote in the following aspects:

446 After reviewing the leading studies on the atmospheric moisture transport
447 *versus* precipitation in the TP, the majority focused on the diagnosis of atmospheric
448 moisture budget and its impact on the precipitation variability in summer, or

449 warm period. Overall, the water vapor from the southern and western boundaries
450 regulates the yearly variability of summer precipitation in the TP. Considered that
451 snowfall or snow-melting process has significant influence on the water resources,
452 as well as the thermal regimes of frozen ground over the TP ([Kang et al., 2010](#);
453 [Yang et al., 2014](#); [Zhang and Ma, 2018](#)), more attention is needed for the
454 atmospheric moisture budget in winter or cold-season. First of all, the physical
455 mechanism for the precipitation variability in winter over the TP is unclear. Some
456 studies have explored the close linkage between the atmospheric moisture
457 transport and precipitation variability in the TP on daily to longer time scales. The
458 sub-daily or hourly scale has not been examined in this region. But such timescale
459 is of great importance for the featured hourly storms and instantaneous floods in
460 the TP. A deeper understanding of extreme rainfall events, such as occurrence,
461 amount, duration, and frequency, is also necessary and would be beneficial to the
462 hazardous floods in the TP under the changing climate. More evidences have
463 suggested the dominating role of the local moisture recycling in the summer
464 precipitation in the TP ([Curio et al., 2015](#); [Sugimoto et al., 2006](#)). But the role of
465 local moisture recycling on the extreme rainfall remains unknown. Thus, how to
466 develop an integrated physical and statistical framework for the TP concerning the
467 influence of atmospheric moisture transport and the associated circulation
468 patterns on the precipitation variability with respect to the various aspects
469 mentioned above is an urgent task.

470 Currently, the analysis data from either satellite retrieval, reanalysis model
471 simulation or field *in-situ* observation are not sufficient to capture complex terrains
472 of the TP, higher spatial resolution products are in great demand to improve the

473 understanding of the moisture transport and assist further quantitative analysis
474 on its linkage / contribution with / to precipitation variability in the TP. For instance,
475 [Lin et al. \(2018\)](#) investigated the spatial resolution dependency of simulated
476 moisture transport through the central Himalayas and its further influence on
477 precipitation bias over the TP. Moreover, the ground-based monitoring network
478 is sparse in the TP, especially in the west, which induces higher uncertainty for the
479 precipitation patterns ([Ma et al., 2015](#)). [Maussion et al. \(2014\)](#) demonstrate the
480 contribution of using the dynamical downscaling approach to produce a better
481 product. We have developed ensemble precipitation data sets with higher quality
482 at daily and 0.25° scales from 2001 to 2015 over the TP ([Ma et al., 2018a](#); [Ma et al.,](#)
483 [2018b](#)), but more efforts need to be done to provide more reliable data sets for our
484 planned work in this region.

485 Conventional “upslope” route is the mainstream hypothesis for the
486 atmospheric moisture transport through the Himalayas and thus into the southern
487 TP ([Xu et al., 2014](#)). Recently, a new “up-and-over” scheme for the atmospheric
488 moisture transport was proposed and evidenced in the southwestern TP ([Dong et](#)
489 [al., 2016](#)). Sensitivity simulations showed that the “upslope” and “up-and-over”
490 routes coexist in the moisture transport processes, where the “upslope” moisture
491 transport is frequent but inefficient, the “up-and-over” transport is more efficient
492 but less frequent ([Dong et al., 2016](#)). However, the detailed moisture transport (e.g.,
493 the transient eddies) is not yet being well described. And the question of how to
494 quantifying the relative contribution of the two modes along the southern slope of
495 Himalayas remains unanswered.

496 The applicable prospect of this review study potentially links the current
497 leading “Sky-River” project in the Three-River Headwaters region, which is
498 regarded as the prominent water resources management program in mainland
499 China ([Wang et al., 2016](#)). One of the great challenge is conducting trans-regional
500 water diversion from the atmospheric rivers at the optimal moment. The artificial
501 precipitation experiment is more empirical and lack of reasonable evaluation and
502 guidance. If the atmospheric moisture transport conditional on the precipitation
503 patterns, especially the extreme rainfall events, were explicitly illustrated, it would
504 be beneficial for the artificial rainfall experiment and thus contributed to this
505 enormous project. In summary, the endeavor for understanding the role of the
506 atmospheric moisture transport and the associated circulation patterns on the
507 precipitation variability in the TP is significantly valuable for the scientific
508 community.

509 **4 Concluding summary**

510 The TP is the highest and one of the most active centers in the global water
511 cycle. Recent processes and challenges regarding the atmospheric moisture
512 transport *versus* precipitation variability across the TP are comprehensively
513 reviewed in this paper.

514 The TP serves as a strong “dynamic pump” and continuously attracts moist air
515 from the surrounding oceans under the large-scale atmospheric circulations. More
516 specifically, the warm-moist air continuously elevates along the southern slope of
517 the Himalayas, where the conventional “upslope” and new-finding “up-and-over”
518 schemes coexist to force the water vapor transport. Although four approaches (i.e.,
519 IWV, IVT, TMEs, and water isotopes) are widely adopted for the identification of

520 atmospheric moisture transport, it is not easy to quantify the role of atmospheric
521 moisture transport on the precipitation in the TP. Based on the moisture budget
522 method, local moisture recycling has larger contribution to the TP's precipitation
523 than that from the remote moisture transport. Overall, the water vapor from the
524 outside is mainly from the southern and western borders, which are driven by the
525 Indian monsoon and the Westerlies, respectively. The water vapor from the
526 western boundary primarily influences the variability of summer rainfall in the
527 southern TP, in spite of weaker amounts than that from the southern boundary.

528 Quantitative identification for the atmosphere moisture sources using the
529 integrated trajectory approach is the next step for exploring the extreme
530 precipitation in the TP. More importantly, a statistical-physical framework aimed
531 to explore the influence of atmospheric moisture transport and associated large-
532 scale circulation patterns on the TP's precipitation should be proposed in advance.
533 Also, it is necessary to develop the atmospheric moisture and precipitation data
534 sets with high accuracy in order to perform the above analysis.

535 **Acknowledgements**

536 This work is financially supported by the National Natural Science Foundation of
537 China (Nos. 41601065, 91437214, and 51709051) and the Hong Kong Research
538 Grants Council funded project (No. 26200017). Y. Ma is partially supported
539 through The Hong Kong University of Science and Technology (HKUST) Post-
540 Doctoral Fellowship (PDF) Matching Fund 2017. M. Lu and M. Pan are partially
541 supported by the HKUST funds (Nos. Z0488, R9392 and IGN16EG06). We would
542 like to thank the Editor and two anonymous reviewers for their thoughtful
543 comments.

544 **References**

- 545 Bhatt, B.C., Nakamura, K., A climatological-dynamical analysis associated with
546 precipitation around the southern part of the Himalayas, *Journal of*
547 *Geophysical Research* **111**(2006), p. D02115.
- 548 Bolch, T. *et al.*, The state and fate of Himalayan glaciers, *Science* **336**(2012), pp.
549 310-314.
- 550 Cai, Z., Tian, L., Atmospheric controls on seasonal and interannual variations in
551 the precipitation isotope in the East Asian monsoon region, *Journal of*
552 *Climate* **29**(2016), pp. 1339-1352.
- 553 Cannon, F. *et al.*, The influence of tropical forcing on extreme winter precipitation
554 in the western Himalaya, *Climate Dynamics* **48**(2016), pp. 1213-1232.
- 555 Chen, B., Xu, X.-D., Yang, S., Zhang, W., On the origin and destination of
556 atmospheric moisture and air mass over the Tibetan Plateau, *Theoretical*
557 *and Applied Climatology* **110**(2012), pp. 423-435.
- 558 Cherchi, A., Navarra, A., Influence of ENSO and of the Indian Ocean Dipole on
559 the Indian summer monsoon variability, *Climate Dynamics* **41**(2012), pp.
560 81-103.
- 561 Chow, K.C., Chan, J.C.L., Diurnal variations of circulation and precipitation in
562 the vicinity of the Tibetan Plateau in early summer, *Climate Dynamics*
563 **32**(2008), pp. 55-73.
- 564 Curio, J., Maussion, F., Scherer, D., A 12-year high-resolution climatology of
565 atmospheric water transport over the Tibetan Plateau, *Earth System*
566 *Dynamics* **6**(2015), pp. 109-124.

567 Dettinger, M.D., Ralph, F.M., Das, T., Neiman, P.J., Cayan, D.R., Atmospheric
568 Rivers, Floods and the Water Resources of California, *Water* 3(2011), pp.
569 445-478.

570 Donat, M.G., Lowry, A.L., Alexander, L.V., O’Gorman, P.A., Maher, N., More
571 extreme precipitation in the world’s dry and wet regions, *Nature Climate*
572 *Change* 6(2016), pp. 508-513.

573 Dong, W. *et al.*, Summer rainfall over the southwestern Tibetan Plateau
574 controlled by deep convection over the Indian subcontinent, *Nat Commun*
575 7(2016), p. 10925.

576 Draxler, R.R., Hess, G.D., An overview of the HYSPLIT_4 modeling system of
577 trajectories, dispersion, and deposition, *Australian Meteorological Magazine*
578 47(1998), pp. 295-308.

579 Duan, A., Li, F., Wang, M., Wu, G., Persistent Weakening Trend in the Spring
580 Sensible Heat Source over the Tibetan Plateau and Its Impact on the Asian
581 Summer Monsoon, *Journal of Climate* 24(2011), pp. 5671-5682.

582 Feng, L., Zhou, T., Water vapor transport for summer precipitation over the
583 Tibetan Plateau: Multidata set analysis, *Journal of Geophysical Research:*
584 *Atmospheres* 117(2012), p. D20114.

585 Gao, Y.C., Liu, M.F., Evaluation of high-resolution satellite precipitation products
586 using rain gauge observations over the Tibetan Plateau, *Hydrology and*
587 *Earth System Sciences* 17(2013), pp. 837-849.

588 Gershunov, A., Shulgina, T., Ralph, F.M., Lavers, D.A., Rutz, J.J., Assessing the
589 climate-scale variability of atmospheric rivers affecting western North
590 America, *Geophysical Research Letters* 44(2017), pp. 1-9.

591 Gimeno, L., Drumond, A., Nieto, R., Trigo, R.M., Stohl, A., On the origin of
592 continental precipitation, *Geophysical Research Letters* **37**(2010), p. L13804.

593 Gimeno, L., Nieto, R., Vázquez, M., Lavers, D.A., Atmospheric rivers: a mini-
594 review, *Frontiers in Earth Science* **2**(2014), pp. 1-6.

595 Gimeno, L. *et al.*, Oceanic and terrestrial sources of continental precipitation,
596 *Reviews of Geophysics* **50**(2012), p. RG4003.

597 Gou, Y., Ma, Y., Chen, H., Wen, Y., Radar-derived quantitative precipitation
598 estimation in complex terrain over the eastern Tibetan Plateau,
599 *Atmospheric Research* **203**(2018), pp. 286-297.

600 Groning, M. *et al.*, A simple rain collector preventing water re-evaporation
601 dedicated for delta O-18 and H-2 analysis of cumulative precipitation
602 samples, *Journal of Hydrology* **448-449**(2012), pp. 195-200.

603 Guo, X., Tian, L., Wen, R., Yu, W., Qu, D., Controls of precipitation $\delta^{18}\text{O}$ on the
604 northwestern Tibetan Plateau: A case study at Ngari station, *Atmospheric*
605 *Research* **189**(2017), pp. 141-151.

606 Hecht, C.W., Cordeira, J.M., Characterizing the influence of atmospheric river
607 orientation and intensity on precipitation distributions over north coastal
608 California, *Geophysical Research Letters* **44**(2017), pp. 9048-9058.

609 Hoffmann, G., Werner, M., Heimann, M., Water isotope module of the ECHAM
610 atmospheric general circulation model: A study on timescales from days
611 to several years, *Journal of Geophysical Research: Atmospheres* **103**(1998), pp.
612 16871-16896.

613 Hou, A.Y. *et al.*, The Global Precipitation Measurement Mission, *Bulletin of the*
614 *American Meteorological Society* **95**(2014), pp. 701-722.

615 Ingram, W., Extreme precipitation: Increases all round, *Nature Climate Change*
616 6(2016), pp. 443-444.

617 Jiang, T., Deng, Y., Downstream modulation of North Pacific atmospheric river
618 activity by East Asian cold surges, *Geophysical Research Letters* 38(2011), p.
619 L20807.

620 Kang, S. *et al.*, Review of climate and cryospheric change in the Tibetan Plateau,
621 *Environmental Research Letters* 5(2010), p. 015101.

622 Knippertz, P., Wernli, H., A Lagrangian Climatology of Tropical Moisture
623 Exports to the Northern Hemispheric Extratropics, *Journal of Climate*
624 23(2010), pp. 987-1003.

625 Knippertz, P., Wernli, H., Gläser, G., A Global Climatology of Tropical Moisture
626 Exports, *Journal of Climate* 26(2013), pp. 3031-3045.

627 Kurita, N., Yamada, H., The Role of Local Moisture Recycling Evaluated Using
628 Stable Isotope Data from over the Middle of the Tibetan Plateau during
629 the Monsoon Season, *Journal of Hydrometeorology* 9(2008), pp. 760-775.

630 Lamjiri, M.A., Dettinger, M.D., Ralph, F.M., Guan, B., Hourly storm
631 characteristics along the U.S. west coast: role of atmospheric rivers in
632 extreme precipitation, *Geophysical Research Letters* 44(2017), pp. 7020-7028.

633 Lavers, D.A., Villarini, G., The nexus between atmospheric rivers and extreme
634 precipitation across Europe, *Geophysical Research Letters* 40(2013), pp. 3259-
635 3264.

636 Lavers, D.A., Villarini, G., Allan, R.P., Wood, E.F., Wade, A.J., The detection of
637 atmospheric rivers in atmospheric reanalyses and their links to British
638 winter floods and the large-scale climatic circulation, *Journal of Geophysical*
639 *Research: Atmospheres* 117(2012), p. D20106.

640 Lin, C., Chen, D., Yang, K., Ou, T., Impact of model resolution on simulating the
641 water vapor transport through the central Himalayas: implication for
642 models' wet bias over the Tibetan Plateau, *Climate Dynamics*(2018).

643 Lin, H., You, Q., Zhang, Y., Jiao, Y., Fraedrich, K., Impact of large-scale
644 circulation on the water vapour balance of the Tibetan Plateau in summer,
645 *International Journal of Climatology* **36**(2016), pp. 4213-4221.

646 Liu, H. *et al.*, Impact of the North Atlantic Oscillation on the Dipole Oscillation of
647 summer precipitation over the central and eastern Tibetan Plateau,
648 *International Journal of Climatology* **35**(2015), pp. 4539-4546.

649 Liu, X., Yin, Z.-Y., Spatial and temporal variation of summer precipitation over
650 the eastern Tibetan Plateau and the North Atlantic Oscillation, *Journal of*
651 *Climate* **14**(2001), pp. 2896-2909.

652 Lu, M., Hao, X., Diagnosis of the Tropical Moisture Exports to the Mid-Latitudes
653 and the Role of Atmospheric Steering in the Extreme Precipitation,
654 *Atmosphere* **8**(2017), p. 256.

655 Lu, M., Lall, U., Tropical Moisture Exports, Extreme Precipitation and Floods in
656 Northeastern US, *Earth Science Research* **6**(2017), pp. 91-111.

657 Lu, M.Q., Lall, U., Schwartz, A., Kwon, H., Precipitation predictability associated
658 with tropical moisture exports and circulation patterns for a major flood in
659 France in 1995, *Water Resources Research* **49**(2013), pp. 6381-6392.

660 Ma, Y. *et al.*, Performance of Optimally Merged Multisatellite Precipitation
661 Products Using the Dynamic Bayesian Model Averaging Scheme Over the
662 Tibetan Plateau, *Journal of Geophysical Research: Atmospheres* **123**(2018a), pp.
663 814-834.

664 Ma, Y. *et al.*, Similarity and Error Intercomparison of the GPM and Its
665 Predecessor-TRMM Multisatellite Precipitation Analysis Using the Best
666 Available Hourly Gauge Network over the Tibetan Plateau, *Remote*
667 *Sensing* **8**(2016), p. 569.

668 Ma, Y. *et al.*, Comprehensive evaluation of Ensemble Multi-Satellite Precipitation
669 Dataset using the Dynamic Bayesian Model Averaging scheme over the
670 Tibetan plateau, *Journal of Hydrology* **556**(2018b), pp. 634-644.

671 Ma, Y., Zhang, Y., Yang, D., Farhan, S.B., Precipitation bias variability versus
672 various gauges under different climatic conditions over the Third Pole
673 Environment (TPE) region, *International Journal of Climatology* **35**(2015), pp.
674 1201-1211.

675 Maussion, F. *et al.*, Precipitation Seasonality and Variability over the Tibetan
676 Plateau as Resolved by the High Asia Reanalysis*, *Journal of Climate*
677 **27**(2014), pp. 1910-1927.

678 Methven, J., *Offline trajectories: Calculation and accuracy, Technical Report 44,*
679 (1997).

680 Najibi, N., Devineni, N., Lu, M., Hydroclimate drivers and atmospheric
681 teleconnections of long duration floods: An application to large reservoirs
682 in the Missouri River Basin, *Advances in Water Resources* **100**(2017), pp. 153-
683 167.

684 Neiman, P.J., Ralph, F.M., Wick, G.A., Lundquist, J.D., Dettinger, M.D.,
685 Meteorological Characteristics and Overland Precipitation Impacts of
686 Atmospheric Rivers Affecting the West Coast of North America Based on
687 Eight Years of SSM/I Satellite Observations, *Journal of Hydrometeorology*
688 **9**(2008), pp. 22-47.

689 Qiu, J., The third pole, *Nature* **454**(2008), pp. 393-396.

690 Ralph, F.M., Neiman, P.J., Wick, G.A., Satellite and CALJET aircraft observations
691 of atmospheric rivers over the eastern north Pacific ocean during the
692 winter of 1997/98, *Monthly Weather Review* **132**(2004), pp. 1721-1745.

693 Risi, C., Bony, S., Vimeux, F., Jouzel, J., Water-stable isotopes in the LMDZ4
694 general circulation model: Model evaluation for present-day and past
695 climates and applications to climatic interpretations of tropical isotopic
696 records, *Journal of Geophysical Research* **115**(2010).

697 Schuessel, P., Emery, W.J., Atmospheric water vapour over oceans from SSM/I
698 measurements, *International Journal of Remote Sensing* **11**(1990), pp. 753-766.

699 Schoeberl, M.R., Newman, P.A., A multiple-level trajectory analysis of vortex
700 filaments, *J Geophys Res Atmos* **100**(1995), pp. 25801-25815.

701 Shen, Y. *et al.*, Uncertainty analysis of five satellite-based precipitation products
702 and evaluation of three optimally merged multi-algorithm products over
703 the Tibetan Plateau, *International Journal of Remote Sensing* **35**(2014), pp.
704 6843-6858.

705 Singh, P., Nakamura, K., Diurnal variation in summer precipitation over the
706 central Tibetan Plateau, *Journal of Geophysical Research* **114**(2009), p.
707 D20107.

708 Sprenger, M., Wernli, H., The LAGRANTO Lagrangian analysis tool – version
709 2.0, *Geoscientific Model Development* **8**(2015), pp. 2569-2586.

710 Stein, A.F. *et al.*, NOAA's HYSPLIT Atmospheric Transport and Dispersion
711 Modeling System, *Bulletin of the American Meteorological Society* **96**(2015),
712 pp. 2059-2077.

713 Stohl, A., Computation, accuracy and applications of trajectories-a review and
714 bibliography, *Atmospheric Environment* **32**(1998), pp. 947-966.

715 Sturm, K., Hoffmann, G., Langmann, B., Stichler, W., Simulation of $\delta^{18}\text{O}$ in
716 precipitation by the regional circulation model REMOiso, *Hydrological*
717 *Processes* **19**(2005), pp. 3425-3444.

718 Sugimoto, S., Ueno, K., Sha, W., Transportation of water vapor into the Tibetan
719 Plateau in the case of a passing synoptic-scale trough, *Journal of the*
720 *Meteorological Society of Japan* **86**(2006), pp. 935-949.

721 Tang, M., Reiter, E.R., Plateau monsoons of the northern hemisphere: a
722 comparison between North America and Tibet, *Monthly Weather Review*
723 **112**(1984), pp. 617-637.

724 Tian, L. *et al.*, Stable isotopic variations in west China: A consideration of
725 moisture sources, *Journal of Geophysical Research* **112**(2007), p. D10112.

726 Tian, L., Yao, T., Numaguti, A., Duan, K., Relation between stable isotope in
727 monsoon precipitation in southern Tibetan Plateau and moisture transport
728 history, *Science In China (Series D)* **44**(2001), pp. 267-274.

729 Tong, K., Su, F., Yang, D., Zhang, L., Hao, Z., Tibetan Plateau precipitation as
730 depicted by gauge observations, reanalyses and satellite retrievals,
731 *International Journal of Climatology* **34**(2014), pp. 265-285.

732 Trenberth, K.E., Changes in precipitation with climate change, *Climate Research*
733 **47**(2011), pp. 123-138.

734 Ueno, K., Toyotsu, K., Bertolani, L., Tartari, G., Stepwise Onset of Monsoon
735 Weather Observed in the Nepal Himalaya, *Monthly Weather Review*
736 **136**(2008), pp. 2507-2522.

737 van der Ent, R.J., Savenije, H.H.G., Schaefli, B., Steele-Dunne, S.C., Origin and
738 fate of atmospheric moisture over continents, *Water Resources Research*
739 **46**(2010), p. W09505.

740 Waliser, D. *et al.*, The “year” of tropical convection (May 2008-April 2010) climate
741 variability and weather highlights, *Bulletin of the American Meteorological*
742 *Society* **93**(2012), pp. 1189-1218.

743 Wang, G. *et al.*, Sky River: Discovery, concept, and implications for future
744 research, *SCIENTIA SINICA Technologica* **46**(2016), pp. 649-656.

745 Wang, X., Pang, G., Yang, M., Precipitation over the Tibetan Plateau during
746 recent decades: a review based on observations and simulations,
747 *International Journal of Climatology*(2017a).

748 Wang, Z., Duan, A., Yang, S., Ullah, K., Atmospheric moisture budget and its
749 regulation on the variability of summer precipitation over the Tibetan
750 Plateau, *Journal of Geophysical Research: Atmospheres* **122**(2017b), pp. 614-
751 630.

752 Werner, H., Davies, H.C., A Lagrangian-based analysis of extratropical cyclones.
753 I: The method and some applications, *Quarterly Journal of the Royal*
754 *Meteorological Society* **123**(1997), pp. 467-489.

755 Wernli, H., A Lagrangian-based analysis of extratropical cyclones. II: A detailed
756 case-study, *Quarterly Journal of the Royal Meteorological Society* **123**(1997),
757 pp. 1677-1706.

758 Wu, G. *et al.*, Thermal controls on the Asian summer monsoon, *Sci Rep* **2**(2012), p.
759 404.

760 Wu, G. *et al.*, The Influence of Mechanical and Thermal Forcing by the Tibetan
761 Plateau on Asian Climate, *Journal of Hydrometeorology* **8**(2007), pp. 770-789.

762 Xu, X., Lu, C., Shi, X., Gao, S., World water tower: An atmospheric perspective,
763 *Geophysical Research Letters* **35**(2008).

764 Xu, X. *et al.*, An important mechanism sustaining the atmospheric "water tower"
765 over the Tibetan Plateau, *Atmospheric Chemistry and Physics* **14**(2014), pp.
766 11287-11295.

767 Yang, K. *et al.*, Recent climate changes over the Tibetan Plateau and their impacts
768 on energy and water cycle: A review, *Global and Planetary Change*
769 **112**(2014), pp. 79-91.

770 Yao, T. *et al.*, A review of climatic controls on $\delta^{18}\text{O}$ in precipitation over the
771 Tibetan Plateau: Observations and simulations, *Reviews of Geophysics*
772 **51**(2013), pp. 525-548.

773 Yao, T. *et al.*, Different glacier status with atmospheric circulations in Tibetan
774 Plateau and surroundings, *Nature Climate Change* **2**(2012), pp. 663-667.

775 You, Q., Kang, S., Aguilar, E., Yan, Y., Changes in daily climate extremes in the
776 eastern and central Tibetan Plateau during 1961–2005, *Journal of*
777 *Geophysical Research* **113**(2008), p. D07101.

778 You, Q., Min, J., Zhang, W., Pepin, N., Kang, S., Comparison of multiple datasets
779 with gridded precipitation observations over the Tibetan Plateau, *Climate*
780 *Dynamics* **45**(2015), pp. 791-806.

781 Zhang, C., Tang, Q., Chen, D., Recent Changes in the Moisture Source of
782 Precipitation over the Tibetan Plateau, *Journal of Climate* **30**(2017), pp.
783 1807-1819.

784 Zhang, Y., Ma, N., Spatiotemporal variability of snow cover and snow water
785 equivalent in the last three decades over Eurasia, *Journal of Hydrology*
786 **559**(2018), pp. 238-251.

787 Zhu, Y., Newell, N.E., Atmospheric rivers and bombs, *Geophysical Research Letters*
788 **21**(1994), pp. 1999-2002.

789 Zhu, Y., Newell, R.E., A proposed algorithm for moisture fluxes from
790 atmospheric rivers, *Monthly Weather Review* **126**(1998), pp. 725-735.

791

792

793

794 **Figure Captions**

795 **Figure 1** A general distribution of (a) composite Integrated Water Vapor (IWV)
796 and (b) vertically horizontal water vapor transport fluxes (IVT) showing the
797 atmospheric moisture transport on Jun 30th 2016 across the globe.

798 **Figure 2** Sketch map of several climate systems that regulates the atmospheric
799 moisture entering the Tibetan Plateau, where the green arrays stand for the Indian
800 monsoon system, the grey arrays stand for the mid-latitude Westerlies, the black
801 arrays stand for the East Asian monsoon system, and the red dotted ellipse stand
802 for the local moisture recycling, also termed as Tibetan Plateau monsoon. The
803 background map shows the mean value of composite Integrated Water Vapor
804 (IWV) and wind direction at 500 *hPa* in the summer of 2016 around the TP.

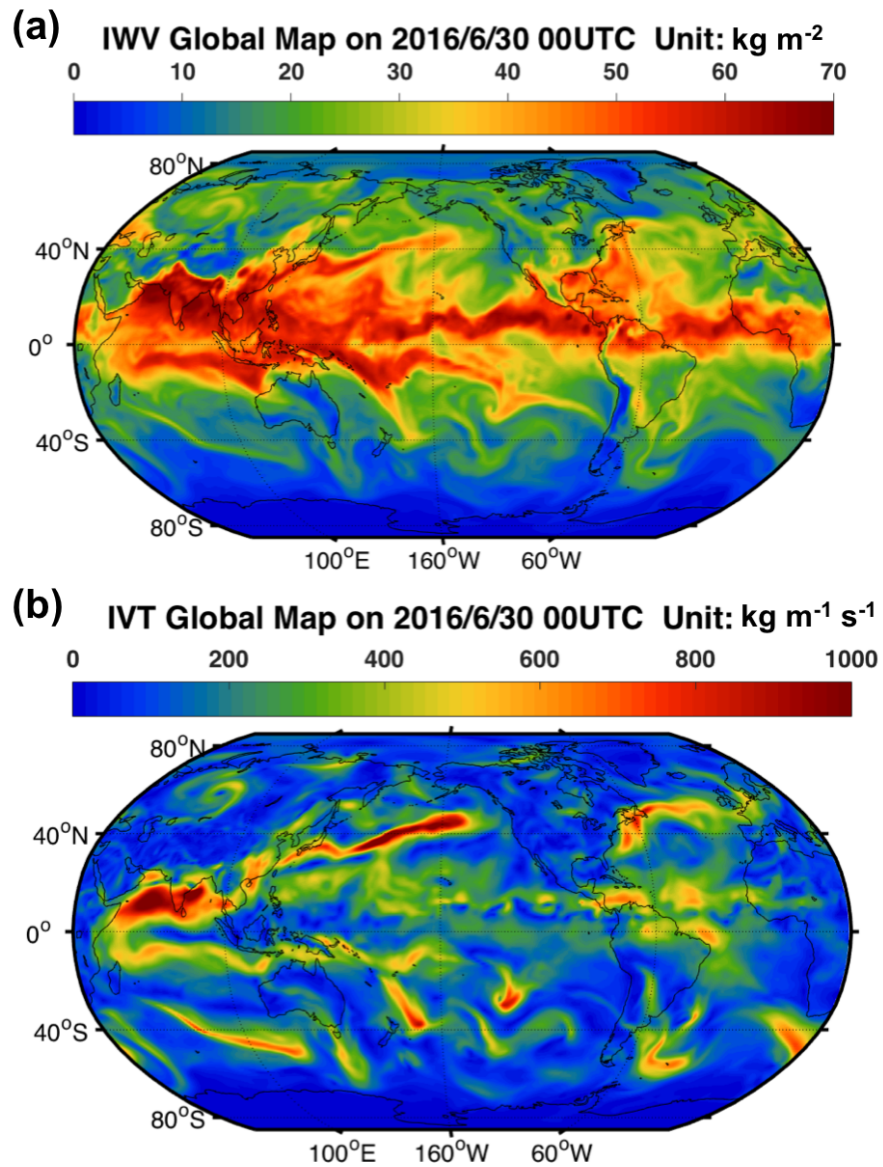
805 **Figure 3** (a) The precipitation $\delta^{18}\text{O}$ monitoring network over the Tibetan Plateau
806 (TP). Red triangles depict locations of $\delta^{18}\text{O}$ monitoring stations, where Up triangles
807 stand for the Global Network of Isotopes in Precipitation (GNIP) stations and
808 down triangles stand for the Tibetan Network for Isotopes in Precipitation (TNIP)

809 stations; Open circles show ice core sites. (b) Schematic framework of the main
810 processes affecting precipitation $\delta^{18}\text{O}$ over the TP. (Cited from Yao et al. (2013))

811 **Figure 4** A diagram of the summary on two ladders of CISK-like processes with
812 two couplings of heat source Q1 and moisture sink Q2 over the southern slopes of
813 TP as well as primary platform in driving atmospheric moisture flows climbing
814 up towards the plateau. (Cited from Xu et al. (2014))

815 **Figure 5** A schematic of the “up-and-over” atmospheric moisture transport from
816 central-eastern India towards the periphery of the southwestern Tibetan Plateau
817 (SWTP) (Cited from Dong et al. (2016))

818



819

820 **Figure 1** A general distribution of (a) composite Integrated Water Vapor (IWB) and (b)
 821 vertically horizontal water vapor transport fluxes (IVT) showing the atmospheric moisture
 822 transport on Jun 30th 2016 across the globe

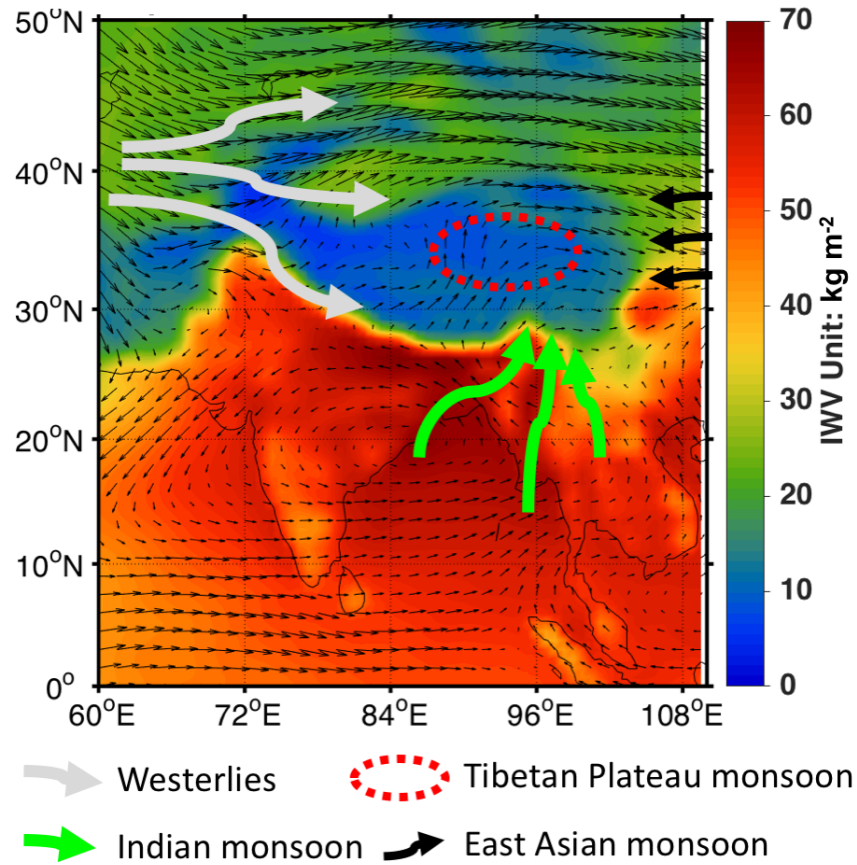
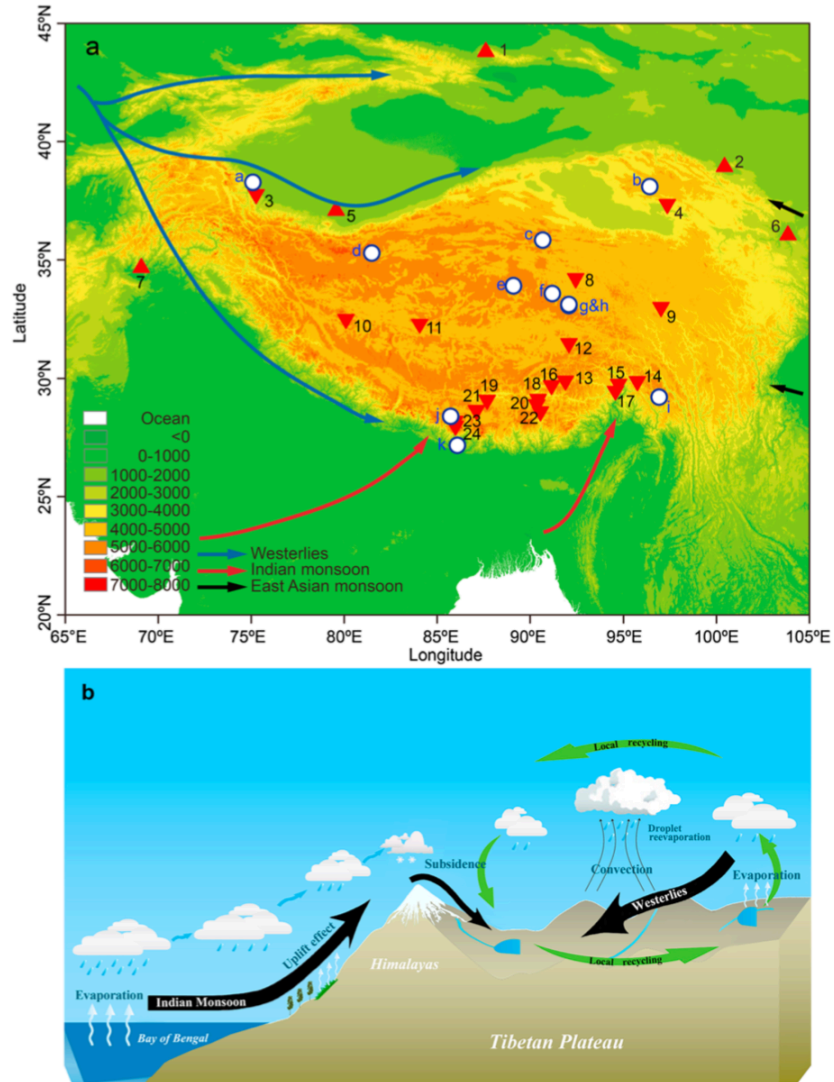


Figure 2 Sketch map of several climate systems that regulates the atmospheric moisture entering the Tibetan Plateau (TP), where the green arrays stand for the Indian monsoon system, the grey arrays stand for the mid-latitude Westerlies, the black arrays stand for the East Asian monsoon system, and the red dotted ellipse stand for the local moisture recycling, also termed as Tibetan Plateau monsoon. The background map shows the mean value of composite Integrated Water Vapor (IWV) and wind direction at 500 *hPa* in the summer of 2016 around the TP.



833

834 **Figure 3** (a) The precipitation $\delta^{18}\text{O}$ monitoring network over the Tibetan Plateau (TP). Red

835 triangles depict locations of $\delta^{18}\text{O}$ monitoring stations, where Up triangles stand for the

836 Global Network of Isotopes in Precipitation (GNIP) stations and down triangles stand for the

837 Tibetan Network for Isotopes in Precipitation (TNIP) stations; Open circles show ice core

838 sites. (b) Schematic framework of the main processes affecting precipitation $\delta^{18}\text{O}$ over the TP.

839

(Cited from Yao et al. (2013))

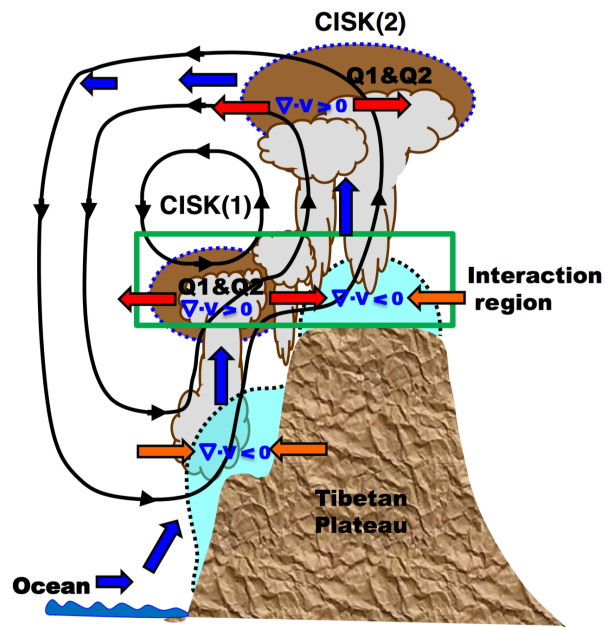
840

841

842

843

844



845

846

847

848

849

Figure 4 A diagram of the summary on two ladders of CISK-like processes with two couplings of heat source Q_1 and moisture sink Q_2 over the southern slopes of Tibetan Plateau (TP) as well as primary platform in driving atmospheric moisture flows climbing up towards the plateau. (Cited from Xu et al., (2014))

850

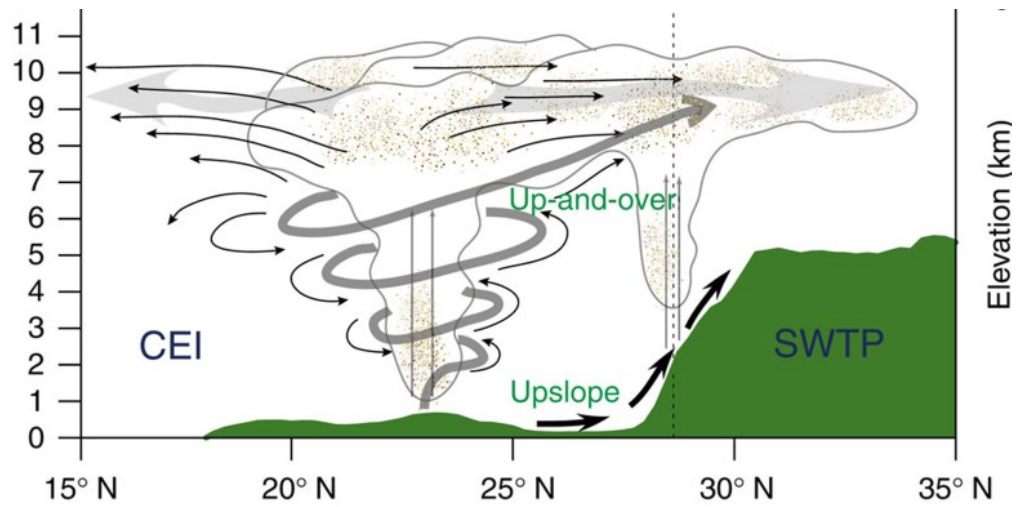
851

852

853

854

855



856

857 **Figure 5** A schematic of the “up-and-over” atmospheric moisture transport from central-
 858 eastern India towards the periphery of the southwestern Tibetan Plateau (SWTP) (Cited from

859

Dong et al. (2016))

860